


ARTICLE OPEN ACCESS

Comparison of Molnupiravir Exposure-Response Relationships for Virology Response and Mechanism of Action Biomarkers With Clinical Outcomes in Treatment of COVID-19

Akshita Chawla¹ | Ruthie Birger¹ | Brian M. Maas¹  | Youfang Cao¹ | Hong Wan¹ | Julie Strizki¹ | Arthur Fridman¹ | Amanda Paschke¹ | Carisa de Anda¹ | Wei Gao¹ | Matthew L. Rizk¹ | Wendy Painter² | Wayne Holman² | Susanne Sardella³ | George Painter⁴ | Julie A. Stone¹

¹Merck & Co., Inc., Rahway, New Jersey, USA | ²Ridgeback Biotherapeutics, Miami, Florida, USA | ³Simulations Plus, Cognigen Corporation, Buffalo, New York, USA | ⁴Emory University School of Medicine, Atlanta, Georgia, USA

Correspondence: Julie A. Stone (julie_stone@merck.com)

Received: 16 January 2025 | **Accepted:** 19 February 2025

Funding: Funding for this research was provided by Merck Sharp & Dohme LLC, a subsidiary of Merck & Co., Inc., Rahway, NJ, USA.

Keywords: β -D-N4-hydroxycytidine | exposure-response | low-frequency nucleotide substitutions | NHC | pharmacokinetics-pharmacodynamics | SARS-CoV-2 | viral load | virologic outcomes

ABSTRACT

Molnupiravir, an orally administered drug for the treatment of mild-to-moderate COVID-19, is a prodrug of the ribonucleoside β -D-N4-hydroxycytidine (NHC). NHC incorporation in the SARS-CoV-2 RNA strand causes an accumulation of deleterious errors in the genome, resulting in reduced viral infectivity and replication. Exposure-response (E-R) analyses for viral RNA mutation rate and virologic outcomes were conducted using data from three phase 2/3 studies of molnupiravir (P006, MOVE-IN, and MOVE-OUT). Three dose levels (200, 400, and 800 mg every 12 hours [Q12H]) and placebo were evaluated. E-R datasets were generated for SARS-CoV-2 RNA mutation and longitudinal SARS-CoV-2 RNA viral load. E-R models were defined for RNA mutation rate and viral load change from baseline at days 5 and 10. The models supported plasma NHC AUC₀₋₁₂ as the appropriate pharmacokinetic driver for assessing E-R relationships. The highest percentage of participants with > 20 low-frequency nucleotide substitutions (LNS) per 10,000 bases, a measure of likely meaningful drug effect, was predicted in the 800 mg Q12H treatment group. A strong drug effect on the reduction of viral load was observed on days 5 and 10. E-R relationships were best represented by an E_{max} structural model with reasonable consistency in the estimated AUC₅₀s (~2.3-fold), across the models, of 10,260 and 4390 nM*hr. for day 5 viral load change from baseline and LNS error rate, respectively. These biomarker E-R curves support the choice of 800 mg Q12H as providing near-maximal drug effect, consistent with findings from the previously published molnupiravir E-R model of clinical outcomes.

Youfang Cao, Hong Wan, and Wei Gao were employees of Merck Sharp & Dohme LLC, a subsidiary of Merck & Co., Inc., Rahway, NJ, USA, at the time of study conduct.

Previous Presentation: This work was presented at the Annual Meeting of the American Society for Clinical Pharmacology and Therapeutics (ASCP); March 22–24, 2023; Atlanta, GA.

This is an open access article under the terms of the [Creative Commons Attribution-NonCommercial](https://creativecommons.org/licenses/by-nc/4.0/) License, which permits use, distribution and reproduction in any medium, provided the original work is properly cited and is not used for commercial purposes.

© 2025 Merck Sharp & Dohme LLC. Ridgeback Biotherapeutics and The Author(s). *Clinical and Translational Science* published by Wiley Periodicals LLC on behalf of American Society for Clinical Pharmacology and Therapeutics.

Summary

- What is the current knowledge on the topic?
 - Molnupiravir, a prodrug of the ribonucleoside β -D-N4-hydroxycytidine (NHC), has demonstrated antiviral activity against SARS-CoV-2 and other RNA viruses by the mechanism of viral error induction—causing an accumulation of transition errors in the viral genome, ultimately leading to the production of a noninfectious virus.
- What question does this study address?
 - How the SARS-CoV-2 RNA mutation rate compares with virologic outcomes in patients treated with molnupiravir at a dose of 200, 400, or 800 mg every 12 hours (Q12H) versus placebo.
- What does this study add to our knowledge?
 - The analyses indicate that at a dose of 800 mg, molnupiravir treatment resulted in the highest percentage of participants with low-frequency nucleotide substitutions, a measure of likely meaningful drug effect, consistent with previously published exposure-response data on molnupiravir.
 - Exposure-dependent reductions in viral load on days 5 and 10 were consistent with the mechanism of action of molnupiravir.
- How might this change clinical pharmacology or translation science?
 - These data support our understanding of the antiviral mechanism of action of molnupiravir and can help inform future development of antiviral treatments against other RNA viruses.

1 | Introduction

Molnupiravir (MK-4482; MOV) is an orally administered ribonucleoside prodrug of β -D-N4-hydroxycytidine (NHC) that has broad-spectrum activity against multiple RNA viruses [1]. In December 2021, MOV received emergency use authorization from the US Food and Drug Administration as a treatment for mild-to-moderate coronavirus disease 2019 (COVID-19) in adults at high risk of progression to severe disease [2]. Following oral administration, MOV is metabolized by esterases to NHC, which is subsequently phosphorylated intracellularly to its pharmacologically active triphosphate anabolite, NHC-TP [1]. NHC-TP is a competitive alternative substrate for the viral RNA-dependent RNA polymerase. Incorporation of NHC in a template strand leads to the accumulation of deleterious mutations in the viral RNA, resulting in inhibition of viral replication and rendering the virus noninfectious [3]. This accumulation of mutations across the viral genome after multiple cycles of viral replication may counteract the potential for resistance mutations to occur, thus contributing to a high barrier to the development of viral resistance to NHC-TP [3, 4]. In clinical trials, MOV 800 mg administered every 12 hours (Q12H) for 5 days was shown to have favorable safety and tolerability in healthy adults as well as in patients with COVID-19 [1, 5]. The exposure-response (E-R) relationship between MOV pharmacokinetics (PK) and clinical outcomes in patients with mild-to-moderate COVID-19 in the MOVE-OUT trial has been previously characterized [6].

Virologic and biomarker data can provide further information on the exposure-dependency of the mechanism of action (MOA) of MOV against severe acute respiratory syndrome coronavirus-2 (SARS-CoV-2) in the clinical setting [7]. Empirical E-R analysis of the virologic and MOA biomarker data played a key role during the interim analyses of phase 2 data to inform the dose selection for phase 3 [8]. This interim analysis was conducted in March 2021 over a short time period to allow for a prompt start of phase 3 given the ongoing global pandemic. At the time, the assumption was made that E-R for these biomarkers would also be informative of the E-R for clinical outcomes, which would be fully informed by phase 3 data.

The aims of the current study were to update the empirical E-R analyses with the full data from the MOV phase 2 and 3 studies to allow for (1) further characterization of exposure-dependency in MOV pharmacodynamic effects and (2) an evaluation of the consistency of E-R modeling results across biomarker-based, virologic, and clinical endpoints. In this manner, the prior assumption around the utility of virologic and MOV biomarkers to inform dose could be fully tested.

2 | Methods

2.1 | Overview

This analysis included data from three MOV clinical trials: P006 ([clinicaltrials.gov](https://clinicaltrials.gov/ct2/show/study/NCT04405570): NCT04405570), MOVE-IN ([clinicaltrials.gov](https://clinicaltrials.gov/ct2/show/study/NCT04575584): NCT04575584), and MOVE-OUT ([clinicaltrials.gov](https://clinicaltrials.gov/ct2/show/study/NCT04575597): NCT04575597) (Table S1). Complete details of all trial designs and results have been previously published [9–11]. All trials were conducted in accordance with an institutional review board–approved protocol, Good Clinical Practice guidelines, and the Declaration of Helsinki. All participants provided written informed consent.

Each study evaluated a placebo arm and three dose levels (200, 400, and 800 mg) of MOV, which provided individual plasma NHC exposures for the purpose of E-R modeling. E-R datasets were generated by merging PK data with clinical data for dosing, baseline covariates, and endpoints from MOVE-IN, MOVE-OUT, and P006. Endpoint data included (1) mutations in SARS-CoV-2 RNA isolated from nasopharyngeal (NP) swabs and (2) longitudinal SARS-CoV-2 RNA viral load data from NP and oropharyngeal swabs. Viral load E-R evaluations focused on NP data because exploratory work suggested that oropharyngeal data had similar patterns of response but greater variability than NP data. Characterization of the E-R relationship from the RNA mutation data obtained from next-generation sequencing to evaluate nucleotide changes in the viral RNA from NP samples from MOV-treated participants and those given placebo provides information on the exposure-dependency of the MOA of MOV against SARS-CoV-2 in the clinical setting.

2.2 | Dataset and Endpoints for E-R Modeling

2.2.1 | SARS-CoV-2 RNA Mutation Rate

The mutation rate datasets were composed of pooled data from MOVE-IN and MOVE-OUT (phase 2 only), where longitudinal

SARS-CoV-2 RNA error counts were obtained from the baseline sequence at days 3 and 5 (end of treatment [EOT]). The data reflect a subset of participants and samples because a viral load of > 600 copies/mL was required to perform the next-generation sequencing assay [7]. No restrictions on time since symptom onset were applied to this dataset.

Two different mutation datasets were prepared for E-R analysis, which differed in terms of variant allele frequency cutoff values. The treatment-emergent single nucleotide variants (TESNV) dataset used a variant allele frequency cut-off value of $\geq 2\%$, and the low-frequency nucleotide substitutions (LNS) dataset used a variant allele frequency between 0.4% and 10%. Because the MOA of MOV is expected to generate widely distributed substitutions in the viral RNA, the LNS dataset with a lower VAF cut-off is expected to better detect the full drug effect and, as such, was considered the primary dataset for the E-R analysis. E-R results from the TESNV dataset were checked for consistency of findings across both datasets.

The following mutation endpoints were considered:

- Number of LNS errors (relative to baseline) and the probability of achieving > 20, >35, and >50 LNS errors per 10,000 nucleotides of SARS-CoV-2 RNA
- Probability of achieving >3, >6, or >9 TESNV mutations per 10,000 nucleotides of SARS-CoV-2 RNA

2.2.2 | Virology

Longitudinal SARS-CoV-2 RNA viral load data in this dataset included observed results as measured by quantitative or qualitative polymerase chain reaction (PCR) at baseline and at days 3, 5 (EOT), 10, 15, and 29 from NP swabs. Only data from nonhospitalized participants with time since symptom onset of ≤ 5 days from MOVE-OUT and P006 were included in this E-R analysis in order to match the inclusion criteria in phase 3 and the labeled usage population (with the exception of the exploratory analysis depicted in Figure S1, which did not implement these data exclusions).

The following virologic endpoints were considered:

- SARS-CoV-2 RNA viral load change from baseline at days 5 (EOT), 10, and 15
- SARS-CoV-2 RNA rate of decline to day 5 (EOT), quantified as a slope (change in \log_{10} copies/mL/day)

2.2.3 | NHC PK Data

Plasma NHC area under the concentration-time curve over the dosing interval (NHC AUC) and trough concentration (C_{trough}) estimates for each participant were obtained from the previously described population pharmacokinetics (PopPK) model [12]. Post hoc plasma NHC AUC and C_{trough} estimates were calculated from simulated day 5 concentration profiles based on PopPK parameters for each participant from MOVE-IN, MOVE-OUT, and P006. Day 5 exposure values are consistent with

steady state. Steady state is reached at day 3; however, because there is very little accumulation of NHC in plasma, values are expected to be a reasonable reflection of exposures across the 5 days of treatment.

2.3 | Model Development

Model structures appropriate for continuous or probabilistic measures, as detailed in the supplement, were applied to the E-R data (Supplementary Methods—Exposure-Response [E-R] Model Structures and Terms).

2.3.1 | Mutation Endpoints E-R Analysis

An exploratory data analysis was conducted to assess the effect of covariates on the efficacy endpoints. The following covariates were assessed: baseline SARS-CoV-2 RNA level, time since symptom onset (categorized as ≤ 5 days and > 5 days), day on which SARS-CoV-2 RNA error counts were measured (day 3 vs. day 5), baseline disease severity, age, sex, body mass index (BMI; kg/m^2), race, and risk factors (yes/no; age > 60 years, active cancer, chronic kidney disease, chronic pulmonary disease, obesity, serious heart conditions, diabetes mellitus).

Both linear and maximum pharmacologic effect (E_{max}) functional forms were explored (starting with linear models) to assess the impact of exposure on the endpoint with a stepwise approach for covariate selection. Guided by the exploratory analysis, baseline viral RNA levels and baseline LNS error counts were assessed as possible covariates in the models.

Model development was guided by a number of criteria to assess the acceptability of a given model. These included successful numerical convergence, objective function value, Akaike information criterion (AIC), acceptable visual predictive check, and acceptable precision of estimated parameters with biologically plausible estimated values. Goodness-of-fit plots (visual predictive check) and simulation-based evaluations were conducted to assess the model performance with regard to prediction of the central tendency and variability of the data.

2.3.2 | Virology Endpoint E-R Analysis

First, a placebo covariate model was built using only the data from participants receiving placebo to avoid potential confounding of covariate relationships with the exposure-dependency in drug effect. Starting with a full covariate model, a stepwise covariate selection (backward elimination) was performed to test for the significance of influential factors. Continuous covariates included baseline viral load (\log_{10} copies/mL), age (years), body weight (kg), and BMI (kg/m^2). Categorical covariates included sex, stratum, disease severity, clade, baseline anti-SARS-CoV-2 antibody status, country, and risk factors (yes/no). If two covariates were highly correlated (e.g., body weight and BMI), then only the strongest univariate covariate was tested. Next, drug and exposure effects were assessed after adding all (MOV plus placebo) data to the model, with the covariate effect terms identified from the placebo data retained in the model

but re-estimated in subsequent steps. Linear and E_{\max} models (where feasible) were used to test for evidence of drug effect. A nonzero slope with respect to NHC exposure was used as evidence of drug effect, and this was tested for NHC AUC and C_{trough} with each endpoint to determine the stronger predictor. AIC and goodness-of-fit plots were used to determine the best model with respect to PK measure and shape of the E-R term. If an E_{\max} model successfully converged and was considered to be a better fit using model selection criteria, additional covariates on E_{\max} were assessed using a forward stepwise selection process, with an entry criterion of $p < 0.05$.

2.4 | Simulations

Simulations were used to characterize the uncertainty around the true E-R effect size for various MOV doses. The dose-response profile for all continuous endpoints was constructed using the final PopPK model and the E-R models for the virology-related endpoints to help inform the therapeutic window of MOV. The simulations aimed to illustrate the true drug effect, taking into account the covariate distribution and the uncertainty in the E-R parameters. For each participant in the analysis dataset, post hoc parameters from the final PopPK model were used to calculate the exposures for the desired dose. An E-R model parameter vector from the bootstrap analysis was drawn. MOV effects on LNS error rate and virology-related endpoints were simulated for each participant in the analysis dataset. These steps were carried out a thousand times for each dose level, and the results were summarized.

All exploratory analyses, models, or diagnostic graphs were performed using R, version 3.0 or later.

3 | Results

3.1 | Mutation Endpoint Analysis

3.1.1 | Exploratory Analysis

Longitudinal SARS-CoV-2 RNA error counts were obtained from baseline sequences on days 3 and 5 (EOT). The LNS error count increased over time in the active treated arms, with a trend toward a greater number of mutations at higher doses, while changes in error count in the placebo arm were minimal (of note, baseline error count in the MOVE-OUT placebo arm was high relative to other arms, but did not increase much during the trial) (Table S2). Binary endpoints based on achievement of error rates defined by thresholds of 20, 35, and 50 mutations per 10,000 nucleotides (relative to baseline) followed a similar trend of dose- and time-dependency as the continuous count measures (Table S3).

E-R analysis. A summary of the key model runs for the LNS error counts, relative to baseline, is shown in Table S4. AUC and C_{trough} were evaluated as linear predictors of response. A significant drug effect was seen when using AUC as the metric in Run 1 (versus Run 1a where C_{trough} is considered as the exposure metric); however, the exposure dependency using data only from MOV arms was not significant (Run 2). This indicated that C_{trough} is a weaker predictor of response compared with AUC.

As seen from the exploratory analysis, the LNS error count increased significantly over time; therefore, day was included as a factor covariate in the model and was subsequently identified as a significant covariate. There was a strong association between LNS error counts and viral RNA levels; therefore, viral load was also identified as a significant covariate. AUC, day, and viral load were identified as significant covariates using the linear functional form. A sigmoidal E-R relationship (E_{\max} model) was explored using the same covariates, and the day variable was shown to be more significant when included as a covariate on E_{\max} instead of baseline pharmacologic effect (E_0). This model indicated that the maximal drug effect was higher on day 5 than on day 3. An E_{\max} model with baseline viral load effect on E_0 and day effect on E_{\max} was considered as the final model for LNS error counts, relative to baseline (Table S4). Final parameter estimates for the LNS E-R model are shown in Table 1. Simulations from the final model demonstrated evidence of a drug effect on days 3 and 5, which at 400mg is nearing the plateau and at 800mg is on the plateau (Figure S2) of the E-R relationship.

As described in the endpoints of interest, LNS error data were also categorized into a binary response (yes/no) using three different thresholds: > 20 , > 35 , and > 50 errors per 10,000 nucleotides of SARS-CoV-2 RNA relative to baseline. Three separate logistic E-R models were constructed to model the probability of achieving the three different thresholds. A summary of the key model runs for the three different threshold endpoints is shown in Table S5. AUC exposures were assessed as having either a linear or a sigmoidal effect. No other covariates besides exposures were assessed in these models. E_{\max} logistic regression was the final model for all three thresholds. Model predictions for the probability of achieving thresholds of > 20 , > 35 , and > 50 LNS errors per 10,000 nucleotides relative to baseline are shown in Figure 1. All three models showed a significant drug effect, with the exposure effect approaching the plateau at 800mg.

For TESNV mutation E-R analysis, data were evaluated as binary endpoints based on the achievement of error rates defined by thresholds of 3, 6, and 9 mutations (per 10,000 bases relative to baseline) at any of the post-baseline visits. The results were qualitatively similar to those for LNS error data in that a significant drug effect was found, and the exposure relationship to that effect appeared to be saturating as exposures reached those associated with the 800-mg dose, with the exception of > 3 TESNV mutations where a linear relationship was found (Figure S3).

TABLE 1 | Final parameter estimates of the final model for LNS error counts relative to baseline.

Term	Estimate	Standard error
E_0	282.3	39.4
VL on E_0	-41.9	5.9
E_{\max} (day 3)	104.7	26.3
E_{\max} (day 5)	243.8	46.5
AUC_{50} (nM*hr)	4447.7	3472.1

Note: AUC_{50} , 50% maximal effective concentration. Abbreviations: E_0 , baseline pharmacologic effect; E_{\max} , maximum pharmacologic effect; E-R, exposure-response; LNS, low-nucleotide substitutions; VL, viral load.

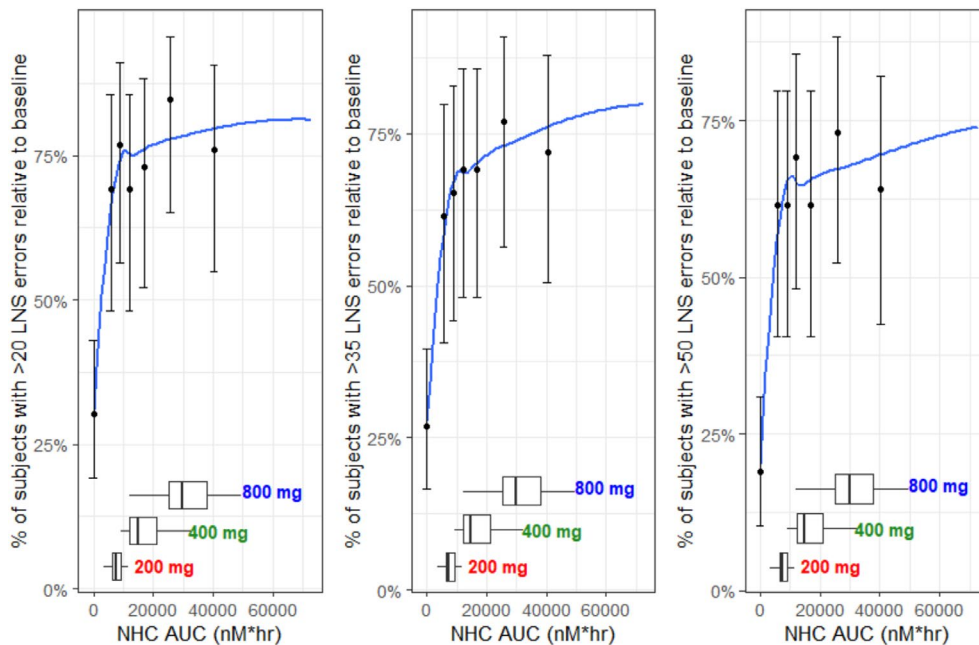


FIGURE 1 | Model-predicted probability of > 20, > 35, and > 50 LNS errors per 10,000 nucleotides relative to baseline. Error bars represent a 95% confidence interval. AUC, area under the concentration-time curve; LNS, low-nucleotide substitution; NHC, β -D-N4-hydroxycytidine.

3.2 | Virology Endpoint Analysis

3.2.1 | Exploratory Analysis

The time since symptom onset of ≤ 5 days inclusion criteria was implemented in the phase 3 study but not in the phase 2 study. This decision was based on the following exploratory virologic dose-response findings at the time of phase 3 dose selection.

In assessments of mean viral load change from baseline stratified by days, both the 400- and 800-mg curves fall below the placebo curve in the groups defined by time since symptom onset 0–3 and 4–5 days, while for the 6- to 7- and 8- to 11-day groups, the 800-mg curve is similar to that of placebo (Figure S1). These results suggest that drug effect and dose response are stronger in the subpopulation with shorter time since symptom onset (TSSO ≤ 5 days). Based on these results, a cutoff of ≤ 5 days was implemented in phase 3 and subsequently, the E-R modeling reported here will be limited to this population (phase 2 data from TSSO > 5 days excluded). In the hospitalized population and among those with a longer time since symptom onset, the limited drug or exposure effects may have been due to a low baseline viral load limiting the ability to detect drug effect, if present. Additionally, the length of time since the start of the infection corresponds to a period in most individual infections where the natural immune response was already clearing the infection and virus; thus, the MOA of MOV may have had limited effects at this stage of the infection.

3.2.2 | E-R Analysis

In the phase 3 MOVE-OUT trial, 756 participants received placebo, while 797 participants received MOV doses ranging from 200 to 800 mg Q12H (Table S6).

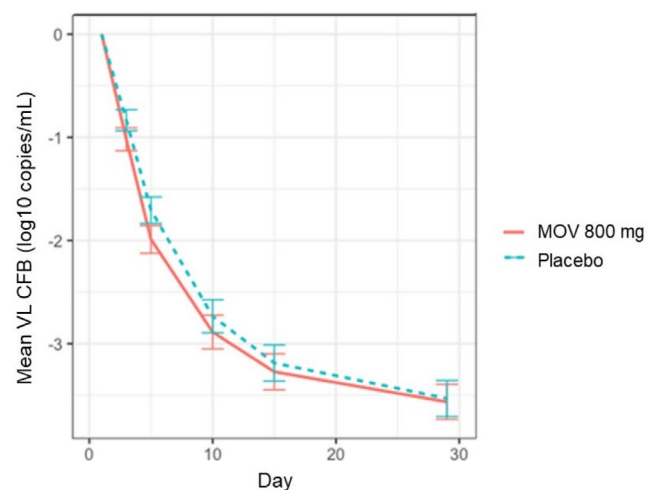


FIGURE 2 | Change from baseline SARS-CoV-2 RNA over time in the phase 3 population. NP, nasopharyngeal; SARS-CoV-2, severe acute respiratory syndrome coronavirus 2; VL, viral load.

The mean viral load change from the baseline profile in the MOV arm generally fell lower than that in the placebo arm, especially in the 3- to 15-day post-treatment range, suggesting an antiviral effect of MOV (Figure 2). The potential for the covariates to be influential factors on the viral load profile was explored, with the aim to identify potential confounders that would need to be accounted for in interpreting the E-R relationships. An important observation was the relationship between baseline viral load and change from baseline viral load at day 5, where data falling along the diagonal are at the theoretical maximal observable viral load decrease based on the lower limit of quantification of the assay (Figure S4). Owing to its strong effect on the change in viral load, baseline viral load was included as a covariate effect in all E-R models developed.

The distribution of baseline viral load with other covariates was explored. Differing clades (Figure S5) had similar baseline viral load, with a trend toward modestly higher values for gamma relative to delta and mu. The unassigned clade category largely reflects baseline samples with low viral load, which did not allow for clade identification.

Participants with a positive antibody status had a lower baseline viral load (Figure S6). Baseline viral load was balanced across the different categories of baseline disease severity (Figure S7). The stepwise covariate selection process allows for the potential effects of these covariates beyond just differences in baseline viral load to be assessed.

Exploration of E-R relationships, by AUC decile plots, in the viral load change from baseline showed an apparent enhanced viral load decrease with increasing MOV exposure on days 5 and 10 (Figure S8). This apparent trend would be tested for significance during formal model development.

3.2.3 | Day 5 Viral Load Change From Baseline

A summary of the key model runs for the placebo and treatment models for day 5 viral load change from baseline is provided in Tables S7 and S8, respectively. A linear model with covariates for baseline viral load and baseline drug severity best described the day 5 change in viral load in patients receiving placebo. Next, MOV-treated participants were added to the dataset used in modeling, and the effects of baseline viral load and baseline disease severity were re-estimated. AUC showed a stronger association with viral load change from baseline and was therefore considered the PK driver for further model development. An E_{\max} drug effect term was selected over a linear term as it was a better representation of the pattern seen in the exploratory data analysis and may better capture physiology as compared with the linear structure. The presence of diabetes was associated with a reduction in drug effect and was included as an additive effect on the E_{\max} term in the final E-R model. Final model parameter estimates are summarized in Table 2. Estimated covariate effects additive on the intercept (E_0) of 1.943 for baseline viral load and baseline disease severity were similar to those obtained in the placebo-only model. The 50% maximal effective concentration (AUC_{50}) was estimated to be 10,260 nM*hr. The model-predicted viral load change from baseline on day 5 is shown in Figure 3.

Day 10 viral load change from baseline. A similar E-R model development approach was used for viral load change from baseline on day 10, where baseline viral load and baseline disease severity were identified as the key covariates in predicting the viral load change. MOV data were subsequently included in the model, and PK drivers and model structures were assessed. Both baseline viral load and baseline disease severity appeared to have a stronger impact on day 10 viral load change from baseline, compared with day 5. The linear model was selected over the E_{\max} model due to AUC being a strong driver of response and showing more favorable Bayesian information criteria compared with the E_{\max} model (Table S9). Final model parameter estimates are summarized in Table S10, and the model-predicted viral change from baseline on day 10 is shown in Figure 3.

TABLE 2 | Final model parameter estimates for the E-R model of viral load change from baseline on day 5.

Term	Estimate	Standard error
E_0	1.943	0.181
bVL	−0.506	0.015
bDS = “Mild”	−0.497	0.155
bDS = “Moderate”	−0.324	0.156
E_{\max}	−0.445	0.207
AUC_{50}	10262.543	18320.328
Additive covariates on E_{\max}		
Diabetes “Yes”	0.707	0.349

Note: AUC_{50} , 50% maximal effective concentration.
Abbreviations: bDS, baseline disease severity; bVL, baseline viral load; E_0 , baseline pharmacologic effect; E_{\max} , maximum pharmacologic effect.

3.2.4 | Analysis for Other Measures of Viral Load Reduction

No models that were evaluated provided a statistically significant relationship between exposure and viral load change from baseline at day 15. This is likely because most participants had a low or undetectable viral load by this visit. Similarly, after accounting for significant covariates in the placebo model, exposure metrics were determined to not have a significant impact on the slope of viral load decline through day 5 ($p > 0.5$). Further development of both models was stopped.

3.2.5 | Simulations: Viral Load Change From Baseline on Day 5

The model-simulated dose–response relationship for the virology endpoint of day 5 viral load change from baseline showed an initial steeper decline in viral load (relative to placebo) up to MOV 400 mg, which plateaued at MOV 800 mg and showed little benefit gained at higher doses (Table 3). Evaluation of the model-predicted viral load change from baseline difference from placebo at simulated MOV doses 100–1600 mg Q12H resulted in a predicted viral load change from baseline for MOV 800 mg of $\sim 0.35 \log_{10}$ copies/mL (Table 3).

4 | Discussion

This article describes the development of E-R models from phase 2/3 dose-ranging data from three studies evaluating 5 days of Q12H oral dosing of MOV in patients infected with SARS-CoV-2. E-R models were defined for LNS error count and viral load change from baseline at days 5 and 10. Each endpoint was independently assessed using empirical E-R approaches in order to limit making assumptions about how the various endpoints might be connected for COVID-19, a newly emerged disease at the time of this analysis. All E-R models supported plasma NHC AUC_{0-12} as a stronger predictor of response than C_{trough} and, thus, as the preferred PK parameter for driving response to MOV.

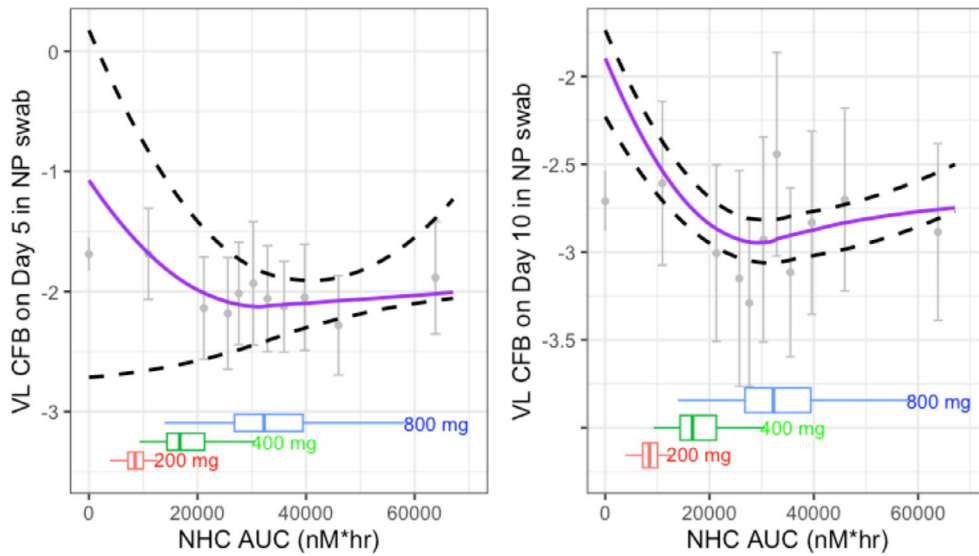


FIGURE 3 | Model-predicted VL change from baseline on days 5 and 10 vs. NHC AUC. A total of 1000 simulations were conducted and summarized to report the median and 2.5th and 97.5th percentiles. The patients were resampled from the analysis dataset, preserving the correlation between exposure and other covariates (baseline disease severity, baseline viral load). Parameter estimates were sampled from the model-estimated variance–covariance matrix to account for uncertainty in estimation. AUC, area under the concentration–time curve; CFB, change from baseline; E-R, exposure–response; NHC, β -D-N4-hydroxycytidine; NP, nasopharyngeal; VL, viral load.

TABLE 3 | Simulated VL CFB (difference from placebo) on day 5 at MOV doses ranging from 100 to 1600 mg Q12H.

Dose (mg)	Day 5 VL CFB (difference from placebo)
	Median (2.5th, 97.5th percentiles)
100	–0.09 (–1.46, 2.00)
200	–0.18 (–1.80, 0.81)
400	–0.26 (–0.94, 0.92)
600	–0.32 (–0.75, 0.16)
800	–0.34 (–0.56, –0.02)
1200	–0.36 (–0.56, –0.04)
1600	–0.38 (–0.59, –0.07)

Abbreviations: CFB, change from baseline; MOV, molnupiravir; Q12H, every 12 hours; VL, viral load.

The MOA of introducing errors into the viral RNA causes an accumulation of substitutions, resulting in the generation of new virions with impaired replication capacity, and thus rendering them noninfectious. For LNS error data, most patients receiving MOV 800 mg achieve exposures associated with near-maximal response. In nonclinical studies of Middle East Respiratory Syndrome, an estimated 10–30 mutations per genome result in robust viral inhibition, with a threefold increase in the mutation rate resulting in a 138-fold decrease in infectious virus and a 6-fold increase resulting in a 26,000-fold reduction in infectious virus [4]. The threshold tests (based on upper 95% confidence interval for effect in placebo for > 20 [day 3] and > 35 [day 5] LNS errors relative to baseline) modeled with the LNS error data were roughly in the highly effective range, as demonstrated by nonclinical data. Simulations utilizing these E-R models indicate that 80% and 75% of patients

receiving MOV 800 mg achieve thresholds of > 20 and > 35 LNS errors relative to baseline, respectively, consistent with meaningful decreases in infectivity. These results are consistent with the MOVE-OUT trial findings of reduced rate of hospitalization/death in patients treated with MOV 800 mg [11] and the absence of infectious virus by day 3 after initiation of therapy [7]. The combination of the high rate of viral mutations reducing viral fitness and the absence of shedding of infectious virus suggests that transmission of a mutated virus from a MOV-treated individual to an uninfected individual is unlikely.

There was strong statistical evidence of an E-R relationship in viral load change from baseline on days 5 and 10. The drug effect on reduction of viral load on day 10 was similar to that seen on day 5, indicating persistence of effects after EOT (day 5), which may in part be due to the longer $t_{1/2}$ of active NHC-TP metabolite in peripheral blood mononucleocytes (13.6–18.0 h) but also likely reflects some additional durability of the virologic pharmacodynamics [13]. Longer times after treatment end (day 15) had weaker evidence for E-R, possibly due to washout of drug effect or viral load at that stage post-infection being too low to demonstrate a drug effect.

The E-R curves were compared using an overlay of normalized E-R curves for the day 5 viral load change from baseline and LNS error rate response measures, as well as with that of the previously evaluated primary clinical outcomes (death/hospitalization) in phase 3 studies [6] (Figure 4). All of these E-R relationships were best represented by an E_{\max} structural model with reasonable consistency in the estimated AUC_{50s} (within ~ 4.5 -fold), across the models of 19,900, 10,260, and 4390 nM*hr for hospitalization/death, day 5 viral load change from baseline, and LNS rate, respectively. Of note, the E_{\max} relationship for hospitalization/death was implemented in a logistic regression model to predict the probability of a binary outcome, unlike the continuous biomarker

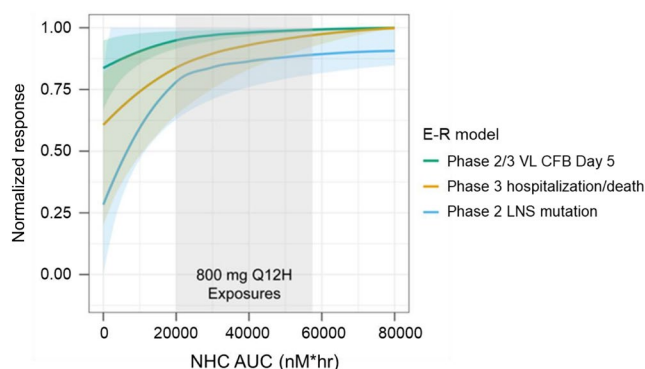


FIGURE 4 | Normalized E_{\max} E-R relationships established for day 5 VL CFB (phase 2 and phase 3) LNS error count (phase 2) and phase 3 clinical outcomes (hospitalization/death) compared with AUC distribution at 800mg Q12H from results of the PopPK model. The y-axis is a relative scale (0–1) and reflects the predicted drug effect relative to the model estimated E_{\max} value for each E-R model. Three different efficacy responses were simulated for a range of exposures using their corresponding E-R models. The efficacy was normalized to a [0, 1] scale using a min-max normalization method where the corresponding E_{\max} value is considered maximum efficacy. The red, green, and blue lines and shaded regions show the mean and 90% CI of the drug effect for various efficacy measures. The shaded area corresponds to the 90% prediction interval of NHC AUC values following a 800mg dose of molnupiravir given Q12H. AUC, area under the concentration-time curve; CFB, change from baseline; E-R, exposure-response; LNS, low-frequency nucleotide substitutions; MOV, molnupiravir; NHC, β -D-N4-hydroxycytidine; PopPK, population pharmacokinetic; Q12H, every 12 hours; VL, viral load.

endpoints modeled in this article. This further log transformation likely steepened the resulting E-R curves and may account for the somewhat larger AUC_{50} estimated.

For these data, an E-R pattern of curvature consistent with a saturating drug effect at MOV 800mg exposures was identified (Figure 4). The exposure distributions of the 200- or 400-mg doses fall along the exposure-dependent portions of the E-R curves and, therefore, can be expected to be associated with reduced drug effects relative to 800mg, supporting the choice of 800mg over lower doses. The available results suggest that additional clinical benefit from increased doses higher than 800mg would be modest in magnitude. Overall, the results support the appropriateness of the MOV 800-mg dose choice for the treatment of COVID-19. Importantly, selection of the 800-mg Q12H dose based on exposures from this dose achieving near-maximal drug effect on virology and MOA biomarker E-R also correctly identified the dose and exposure range approaching the plateau of drug effect on clinical outcomes.

There was also considerable consistency in covariate effects identified across response measures. Baseline viral load was included in all E-R models. Baseline disease severity was identified as a significant predictor of virologic outcome (higher viral load with more severe symptoms) and in the previously published clinical outcome [6] (higher risk of hospitalization with more severe symptoms) models. Diabetes was associated with a smaller drug effect on viral load and a greater risk of hospitalization. All of these

findings are consistent with the conventional understanding of factors that increase the risk for severe COVID-19.

Limitations of these analyses include the exclusion of participants for whom PK data were missing or for whom no baseline viral load sample was obtained. Furthermore, there was a lack of mutation and error data from phase 3 MOVE-OUT, phase 2 MOVE-OUT, and MOVE-IN because these assays could only be run in participants with relatively high viral loads. Lastly, the AUC_{50} parameter for the viral load change from baseline model (day 5) was not well estimated; however, an E_{\max} model still provided a better fit to the data than a linear model.

5 | Conclusions

Consistent with the proposed MOA of incorporating errors into the viral genome leading to inhibition of replication, a higher and an exposure-dependent mutation rate across the viral genome was seen in the MOV-treated participants compared with placebo. Exposure-dependent enhanced reductions in viral load on days 5 and 10 were observed with increasing MOV exposures, consistent with the MOA of MOV, leading to effects on viral load. Overall, the E-R results support the administration of MOV 800mg Q12H for the treatment of COVID-19, as this dose provided a substantial drug effect on mutation rate and viral load, and was generally larger than that projected for MOV 200 or 400mg.

Author Contributions

A.C., B.M.M., and J.A.S. wrote the manuscript. A.C., R.B., B.M.M., Y.C., W.G., M.L.R., J.A.S., G.P., and W.H. designed the research. A.C., R.B., B.M.M., Y.C., H.W., W.P., and S.S. performed the research. A.C., R.B., B.M.M., Y.C., J.S., A.F., A.P., C.A., M.L.R., J.A.S., G.P., and W.H. analyzed the data. J.S. and A.F. contributed new reagents or analytical tools.

Acknowledgments

The authors thank all of the participants and their families, nurses, clinical and laboratory personnel, trial coordinators, and operations staff who participated in these studies. We would like to thank Dr. Sindhuri Kondragunta of Simulations Plus for support with data management and analysis dataset creation. Medical writing and/or editorial assistance was provided by Ascentia Seboko, PhD, and Karen Yee, PhD (ApotheCom, London, UK). This assistance was funded by Merck Sharp & Dohme LLC, a subsidiary of Merck & Co. Inc., Rahway, NJ, USA.

Conflicts of Interest

A.C., R.B., H.W., J.S., A.F., Y.C., B.M.M., A.P., C.d.A., W.G., M.L.R., and J.A.S. are/were employees of Merck Sharp & Dohme LLC, a subsidiary of Merck & Co. Inc., Rahway, NJ, USA, and may hold stock or stock options in Merck & Co. Inc., Rahway, NJ, USA. W.H. is an owner and cofounder, and advisor to Ridgeback Biotherapeutics LP, Miami, FL, USA, and is listed as an inventor on patent applications relating to molnupiravir and owns stock and/or stock options in Merck & Co. Inc., Rahway, NJ, USA. W.P. is an employee of Ridgeback Biotherapeutics. S.S. is an employee of Simulations Plus, Cognigen Division, which was contracted by Merck & Co., Inc., Rahway, NJ, USA, to perform the analysis reported here. G.P. receives royalties under the Emory license on the sale of molnupiravir, is listed as an inventor on multiple issued and pending patent applications relating to molnupiravir, and is an advisor to Ridgeback Biotherapeutics LP, Miami, Florida, USA.

References

1. W. P. Painter, W. Holman, J. A. Bush, et al., "Human Safety, Tolerability, and Pharmacokinetics of Molnupiravir, a Novel Broad-Spectrum Oral Antiviral Agent With Activity Against SARS-CoV-2," *Antimicrobial Agents and Chemotherapy* 65 (2021): e02428-20.
2. U. S. Food and Drug Administration. "Coronavirus (COVID-19) Update: FDA Authorizes Additional Oral Antiviral for Treatment of COVID-19 in Certain Adults," 2021, <https://www.fda.gov/news-events/press-announcements/coronavirus-covid-19-update-fda-authorizes-additional-oral-antiviral-treatment-covid-19-certain>.
3. M. L. Agostini, A. J. Pruijsenrs, J. D. Chappell, et al., "Small-Molecule Antiviral β -d-N(4)-Hydroxycytidine Inhibits a Proofreading-Intact Coronavirus With a High Genetic Barrier to Resistance," *Journal of Virology* 93 (2019): e01348-19.
4. T. P. Sheahan, A. C. Sims, S. Zhou, et al., "An Orally Bioavailable Broad-Spectrum Antiviral Inhibits SARS-CoV-2 in Human Airway Epithelial Cell Cultures and Multiple Coronaviruses in Mice," *Science Translational Medicine* 12 (2020): eabb5883.
5. S. H. Khoo, R. Fitzgerald, T. Fletcher, et al., "Optimal Dose and Safety of Molnupiravir in Patients With Early SARS-CoV-2: A Phase I, Open-Label, Dose-Escalating, Randomized Controlled Study," *Journal of Antimicrobial Chemotherapy* 76 (2021): 3286–3295.
6. A. Chawla, R. Birger, H. Wan, et al., "Factors Influencing COVID-19 Risk: Insights From Molnupiravir Exposure-Response Modeling of Clinical Outcomes," *Clinical Pharmacology and Therapeutics* 113 (2023): 1337–1345.
7. J. M. Strizki, J. A. Grobler, N. Murgolo, et al., "Virologic Outcomes With Molnupiravir in Non-hospitalized Adult Patients With COVID-19 From the Randomized, Placebo-Controlled MOVE-OUT Trial," *Infectious Disease and Therapy* 12, no. 12 (2023): 2725–2743, <https://doi.org/10.1007/s40121-023-00891-1>.
8. A. Chawla, Y. Cao, J. Stone, et al., "Model-Based Dose Selection for the Phase 3 Evaluation of Molnupiravir (MOV) in the Treatment of COVID-19 in Adults," 31st Annual European Congress of Clinical Microbiology and Infectious Diseases, 2021.
9. J. R. Arribas, M. D. S. Bhagani, S. M. Lobo, et al., "Randomized Trial of Molnupiravir or Placebo in Patients Hospitalized With Covid-19," *NEJM Evidence* 1 (2022): 100044.
10. Y. Caraco, G. E. Crofoot, P. A. Moncada, et al., "Phase 2/3 Trial of Molnupiravir for Treatment of Covid-19 in Nonhospitalized Adults," *NEJM Evidence* 1, no. 2 (2022): 100043, <https://doi.org/10.1056/EVIDoa2100043>.
11. A. Jayk Bernal, "Molnupiravir for Oral Treatment of Covid-19 in Nonhospitalized Patients," *New England Journal of Medicine* 386 (2022): 509–520.
12. S. Bihorel, Y. Cao, A. Chawla, et al., "Population Pharmacokinetics of Molnupiravir in Adults With COVID-19: Lack of Clinically Important Exposure Variation Across Individuals," *CPT: Pharmacometrics & Systems Pharmacology* 12 (2023): 1859–1871.
13. M. Iwamoto, K. E. Duncan, P. K. Wickremasingha, et al., "Assessment of Pharmacokinetics, Safety, and Tolerability Following Twice-Daily Administration of Molnupiravir for 10 Days in Healthy Participants," *Clinical and Translational Science* 16 (2023): 1947–1956.

Supporting Information

Additional supporting information can be found online in the Supporting Information section.